Comparison of the Conformation of Active and Nonactive Backbone Cyclic Analogs of Substance P as a Tool To Elucidate Features of the Bioactive Conformation: NMR and Molecular Dynamics in DMSO and Water

Simona Golic Grdadolnik,[†,§] Dale F. Mierke,[†,⊥] Gerardo Byk,[‡] Irena Zeltser,[‡] Chaim Gilon,[‡] and Horst Kessler*,[†]

Institut für Organische Chemie und Biochemie, Technische Universität München, Lichtenbergstrasse 4, D-85747 Garching, Germany, and Department of Organic Chemistry, The Hebrew University of Jerusalem, I-91904 Jerusalem, Israel

Received December 20, 1993[•]

The conformations of two backbone-cyclized substance P analogs as derived from ^{1}H NMR and molecular dynamics simulations carried out in DMSO and water are described. The method of floating chiralities is used in the simulations to facilitate the diastereotopic assignment of methylene protons. One of the analogs, cyclo-[-$(CH_2)_3$-NH-CO-$(CH_2)_4$-Arg-Phe-Phe-N-]-CH_2-CO-Leu-Met-NH_2, is a highly active, selective agonist for the NK- receptor, while the other, cyclo[-$(CH_2)_2$-NH-CO-$(CH_2)_2$-Gly-Arg-Phe-Phe-N-]-CH_2-CO-Leu-Met-NH_2, is inactive. Both analogs contain cyclic ring systems of the same size, varying in only the number of amide linkages. From the conformational analysis, the lack of activity can be attributed to the introduction of too much constraint into the ring system. This has an effect on the topological array of the important residues Arg-Phe-Phe. The results presented here are compared with biologically active analogs previously examined. The differences between conformations of active and inactive compounds are used to develop insight into the conformational requirements for biological activity.

Introduction

To introduce constraint into the native, linear substance P (SP) peptide, Arg-Pro-Lys-Pro-Gln-Gln-Phe-Phe-Gly-Leu-Met-NH_2, the idea of backbone cyclization has been utilized.[1] Head-to-tail cyclization gave inactive compounds, while backbone cyclization gave highly potent substance P receptor agonists. The cyclization procedure, using linkers based on molecular modeling of linear analogs,[2] has produced analogs that are highly receptor-selective, metabolically stable, and conformationally constrained and, therefore, can be meaningfully examined by NMR and computer simulations.[3]

Recently, we examined the conformation of two members from a series of cyclic SP analogs.[4] The analogs contain a linker of methylene groups and one amide linkage resulting in 18- and 19-membered cyclic systems (Figure 1). SP3 and SP4 were both biologically active, with a very high selectivity for the NK-1 receptor (Table 1).

Here, we report the conformational analysis of two additional analogs of backbone-cyclized SP analogs (see SP1 and SP2, Figure 1). SP2 is highly active and selective for the NK-1 receptor, while SP1 is inactive at all three receptors (Table 1). The two analogs SP1 and SP2 are closely related. The chain -CH_2-CH_2-CH_2-CH_2-CO-Arg- in analog SP2 has been replaced by the chain -CH_2-CO-NH-CH_2-CO-Arg- in analog SP1. Therefore, both analogs have the same sequence, the same location of the ring, and the same ring size (20 atoms). The two analogs differ in the number of methylene groups vs amide bonds in the ring: the inactive analog SP1 has five methylene groups and six amide bonds, whereas the active analog SP2 has six methylene groups and five amide bonds. Also, the relative locations of the methylene groups and the amide bonds in the ring differ in both analogs (Figure 1). The conformations of SP1 and SP2 are then compared with the conformations of the analogs previously examined.

The conformations of SP1 and SP2 are derived from ^{1}H NMR and molecular dynamics (MD) simulations carried out in DMSO and water. A special feature of the structure determination in this paper is the use of floating chiralities, removing the restraints on the methylene protons so that the protons are free to switch prochiral positions during the simulation and then using both NOEs and coupling constants as restraints. Floating chiralities has been shown to be useful for the diastereotopic assignment within proteins,[5] where a large number of NOEs are often available. In the case of peptides, NOEs alone are usually not sufficient to make unambiguous assignments: there are far fewer NOEs in peptides than for proteins because of the larger ratio of surface to core. Here, by incorporating both NOE and coupling constant restraints directly in the simulation,[6-8] the diastereotopic assignment is greatly facilitated.

Results

Nuclear Magnetic Resonance. Both of the cyclic SP analogs (SP1 and SP2) were examined in DMSO. To avoid problems with aggregation, the concentrations were kept as low as possible for NMR examination in a reasonable amount of time (0.7 mM). The biologically active compound, SP2, also was investigated in water.

The proton chemical shifts were assigned following standard procedures[9,10] using TOCSY, P.E.COSY, NOESY, and ROESY spectra. The carbons were assigned using an HMQC spectrum. Two isomers were observed in the spectra of SP1, corresponding to trans and cis isomers about the Phe^3-Gly^4 amide bond in a ratio of 66:34, respectively. Interconversion between both conformers could be observed via exchange cross-peaks in the ROESY spectrum with a mixing time of 200 ms. The chemical

* To whom correspondence should be addressed. Phone: (Germany)-89-32093300. FAX: (Germany)-89-32093210.
† Technische Universität München.
‡ The Hebrew University of Jerusalem.
§ Permanent address: National Institute of Chemistry, Hajdrihova 19, SLO-61000 Ljubljana, Slovenia.
⊥ Present address: Department of Chemistry, Clark University, Worcester, MA 06160.
• Abstract published in *Advance ACS Abstracts*, June 1, 1994.

0022-2623/94/1837-2145$04.50/0

SP1

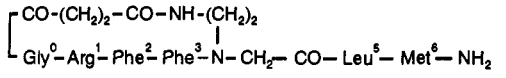

SP2

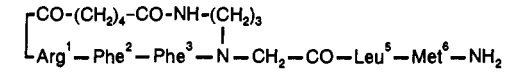

SP3

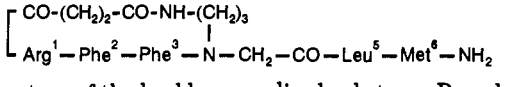

SP4

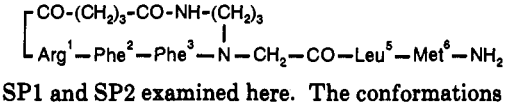

Figure 1. Structure of the backbone-cyclized substance P analogs SP1 and SP2 examined here. The conformations of analogs SP3 and SP4, which were previously studied,[4] are used for the development of structural insight into the requirements of activity at the NK-1 receptor.

Table 1. Biological Activity and Receptor Selectivity of N-Backbone-to-Amino End Cyclic Analogs of Substance P[17]

	biological activity (EC_{50}, nM)		
peptide no.	NK-1	NK-2	NK-3
SP1	>10000	>50000	>10000
SP2	5	>50000	>10000
SP3	180	>50000	>10000
SP4	11	>50000	>10000

shifts are listed in Table 2. The temperature coefficients measured for the amide protons are given in Table 3.

The NOESY spectra were used to calculate interatomic proton–proton distances, using the two-spin approximation and the integrated intensity of a geminal pair of protons assumed to have a distance of 1.78 Å. The distances, listed in Tables 4 and 5, were used in the MD calculations, as discussed below, with +10% and −10% for the upper and lower restraints, respectively. Homonuclear coupling constants were obtained from analysis of P.E.COSY and 1D proton spectra. These values are listed in Table 6.

The differences in the experimental parameters of SP2 in DMSO and water are not significant. The NOEs for the two solvents, included in Tables 4 and 5, are almost identical. The largest difference corresponds to a distance of 0.5 Å, which is not significant considering a modest error of 10% in the calculated distances. The coupling constants, given in Table 6, are also indicative of very minor conformational changes on going from DMSO to water. There are differences up to 1.3 Hz in the backbone couplings, while the couplings within the side chains are almost identical.

Computer Simulations. The MD simulations were carried out in the same solvent as the NMR investigations, DMSO or water. The restraints (NOE and coupling constants) were used for 280 ps of the simulations and then removed (free MD) for 140 ps to examine the quality of the structure. If the conformation developed from the restraints is not energetically favorable, there will be significant conformational changes during the free MD. Our approach using explicit solvent for the MD calculations and performance seems to be more realistic than running long high-temperature MD under unrealistic conditions (in vacuo or continuous DK). However, our limited calculation power prevented a long MD run at high temperature and different starting structures when solvents are included.

The results, illustrated by average dihedral angles, from the restrained and free portions of the MD simulations for the two analogs in DMSO are given in Table 6. The average distance restraint violation from the restrained simulations of SP1 in DMSO is 0.16 Å. There are three distance restraints with violations greater than 0.5 Å: Phe^3H^N–Phe^3H^β, 0.53 Å; Phe^3H^N–Phe^2H^β, 0.59 Å; and Phe^3H^α–II^2H^γ, 0.75 Å. It is important to note that all

Table 2. Proton Chemical Shifts of SP1 in DMSO and SP2 in DMSO and H_2O[a]

	SP1		SP2	
atoms[b]	major	minor	DMSO	H_2O
Gly^0H^N	8.24	8.59		
$Gly^0H^{\alpha1}$	3.93	3.81		
$Gly^0H^{\alpha2}$	3.31	3.37		
Arg^1H^N	8.10	8.03	8.11	8.17
Arg^1H^α	3.95	4.09	3.83	3.90
$Arg^1H^{\beta1}$	1.49 (*pro-R*)	1.73	1.52 (*pro-R*)	1.49
$Arg^1H^{\beta2}$	1.33 (*pro-S*)	1.38	1.40 (*pro-S*)	1.49
$Arg^1H^{\gamma1}$	1.26	1.38	1.34	1.33
$Arg^1H^{\gamma2}$	1.20	1.38	1.27	1.19
Arg^1H^δ	2.95	3.00	2.98	3.02
$Arg^1H^{N\epsilon}$	7.34	7.35	7.41	6.99
Phe^2H^N	7.38	7.62	7.00	7.45
Phe^2H^α	4.59	4.15	4.52	4.63
$Phe^2H^{\beta1}$	3.12 (*pro-S*)	3.05	2.99 (*pro-S*)	3.02
$Phe^2H^{\beta2}$	2.76 (*pro-R*)	2.88	2.77 (*pro-R*)	2.80
Phe^3H^N	8.43	8.07	8.79	8.44
Phe^3H^α	4.83	4.54	4.94	4.78
$Phe^3H^{\beta1}$	2.96	3.03	3.02 (*pro-R*)	3.04
$Phe^3H^{\beta2}$	2.85	2.77	2.87 (*pro-S*)	2.93
$Gly^4H^{\alpha1}$	4.01	4.51	4.08	3.99
$Gly^4H^{\alpha2}$	3.81	3.97	3.75	3.99
Leu^5H^N	7.97	8.37	8.00	8.12
Leu^5H^α	4.29	4.36	4.30	4.29
Leu^5H^β	1.48	1.48	1.48	1.58
Leu^5H^γ	1.62	1.62	1.62	1.58
$Leu^5H^{\delta1}$	0.88	0.88	0.87	0.89
$Leu^5H^{\delta2}$	0.83	0.83	0.84	0.84
Met^6H^N	7.94	8.06	7.93	8.27
Met^6H^α	4.25	4.24	4.27	4.37
$Met^6H^{\beta1}$	1.93	1.87	1.93	2.04
$Met^6H^{\beta2}$	1.80	1.73	1.81	1.96
$Met^6H^{\gamma1}$	2.44	2.39	2.45	2.55
$Met^6H^{\gamma2}$	2.38	2.28	2.38	2.45
Met^6H^ϵ	2.00	1.94	2.01	2.01
$I H^{\alpha1}$	2.50	2.45	2.14	2.23
$I H^{\alpha2}$	2.24	2.29	2.05	2.23
$I H^{\beta1}$	2.45	2.30	1.58	1.50
$I H^{\beta2}$	2.27	2.30	1.25	1.38
$I H^{\gamma1}$			1.58	1.38
$I H^{\gamma2}$			1.39	1.38
$I H^{\delta1}$			2.00	2.18
$I H^{\delta2}$			2.00	2.06
$II H^N$	7.62	7.31	7.67	7.79
$II H^{\alpha1}$	3.19	3.26	3.12	3.18
$II H^{\alpha2}$	3.07	3.26	2.79	2.98
$II H^{\beta1}$	3.51	4.09	1.59	1.67
$II H^{\beta2}$	3.51	2.61	1.48	1.54
$II H^{\gamma1}$			3.36	3.32
$II H^{\gamma2}$			3.26	3.32

[a] Chemical shifts are given in ppm. [b] The low- and high-field protons are indicated with 1 and 2, respectively.

Table 3. Temperature Dependence of the Amide Protons of SP1 and SP2 in DMSO[a]

isomer	Gly^0	Arg^1	Phe^2	Phe^3	Leu^5	Met^6	II
SP1 major	5.1	4.7	0.0	4.7	3.9	5.3	3.8
minor	5.5	5.5	1.6	5.7	6.1	5.5	1.9
SP2		3.7	0.0	4.3	4.6	5.3	6.4

[a] The temperature coefficients are given in negative ppb K^{-1}.

Table 4. Interresidual Distances Calculated from NOESY Spectra of SP1 in DMSO and SP2 in DMSO and H_2O[a]

	SP1		SP2	
atoms	major	minor	DMSO	H_2O
Gly^{0}H^N Arg^{1}H^N		3.1		
Gly^{0}H^N I H$^{\alpha 1}$	2.4	2.4		
Gly^{0}H^N I H$^{\alpha 2}$	2.6	2.5		
Gly^{0}H$^{\alpha 1}$ Arg^{1}H^N	*b*	2.3		
Gly^{0}H$^{\alpha 2}$ Arg^{1}H^N	3.2	2.7		
Gly^{0}H$^{\alpha 2}$ Leu^{5}H^N		3.3		
Arg^{1}H^N Phe^{2}H^N	2.3	2.5	2.6	2.7
Arg^{1}H^N I H$^{\alpha 1}$			2.6 }	2.6[c]
Arg^{1}H^N I H$^{\alpha 2}$			3.1 }	
Arg^{1}H$^\alpha$ Phe^{2}H^N	2.8	2.7	3.7	3.2
Arg^{1}H$^{\beta 1}$ Phe^{2}H^N	3.4		3.6 }	3.4[c]
Arg^{1}H$^{\beta 2}$ Phe^{2}H^N	2.9		3.6 }	
Phe^{2}H^N Phe^{3}H^N	3.5		4.2	
Phe^{2}H^N II H$^{\beta 1}$			3.9	
Phe^{2}H$^\alpha$ Phe^{3}H^N	2.2	2.4	2.4	2.2
Phe^{2}H$^{\beta 1}$ Phe^{3}H^N	2.8			
Phe^{2}H$^{\beta 2}$ Phe^{3}H^N	3.1		3.1	3.2
Phe^{3}H$^\alpha$ II H^N	2.7		3.6	*b*
Phe^{3}H$^\alpha$ II H$^{\alpha 1}$	2.8			
Phe^{3}H$^\alpha$ II H$^{\alpha 2}$	2.3			
Phe^{3}H$^\alpha$ II H$^{\beta 1}$ }	2.1[c]		3.2	2.8
Phe^{3}H$^\alpha$ II H$^{\beta 2}$ }			3.1	3.0
Phe^{3}H$^\alpha$ II H$^\gamma$			*b*	2.2
Gly^{4}H$^{\alpha 1}$ II H$^{\beta 1}$			3.3 }	3.0[c]
Gly^{4}H$^{\alpha 2}$ II H$^{\beta 1}$			3.4 }	
Gly^{4}H$^{\alpha 1}$ II H$^{\beta 2}$			4.4 }	3.3[c]
Gly^{4}H$^{\alpha 2}$ II H$^{\beta 2}$		2.5	3.4 }	
Gly^{4}H$^{\alpha 1}$ II H$^{\alpha 2}$	2.4			
Gly^{4}H$^{\alpha 2}$ II H$^{\alpha 2}$	2.2			
Gly^{4}H$^{\alpha 1}$ II H$^\gamma$			*b* }	2.9[c]
Gly^{4}H$^{\alpha 2}$ II H$^\gamma$			*b* }	
Gly^{4}H$^{\alpha 1}$ Leu^{5}H^N	2.4	2.5	2.8 }	2.6[c]
Gly^{4}H$^{\alpha 2}$ Leu^{5}H^N	2.5	2.3	2.8 }	
Met^{6}H^N Leu^{5}H$^\beta$	3.1	3.4	3.8	3.3
II H^N I H$^{\beta 1}$	2.4	2.8		
II H^N I H$^{\beta 2}$	2.5	2.9		
II H^N I H$^{\delta 1}$ }			2.8[c]	2.8
II H^N I H$^{\delta 2}$ }				2.6

[a] Distances are in A. [b] Distances could not be determined because of the signal overlap. [c] H$^\beta$ are overlapped.

involve the Phe^3 residue. During the restrained simulation, no hydrogen bonds are observed. This is in contrast to the low-temperature coefficient for the Phe^{2}H^N. The calculations of coupling constants, calculated for each structure of the trajectory and then averaged, are in good agreement with the experimental values. The average structure, partially energy minimized to remove some abnormalities from averaging, is given in Figure 3, top.

The free MD simulation of SP1 in DMSO illustrates some conformational changes centered at Phe^2. The ψ of Arg^1 and ϕ of Phe^2 change by $\sim$60°, while the ψ of Phe^2 and ϕ of Phe^3 change by $\sim$150°. These pairs of dihedral angles are coupled, since the ω angle between them is maintained at 180°.

The average distance restraint violation from the restrained simulations of SP2 is 0.14 Å. There is one distance restraint with a violation greater than 0.5 Å: Phe^3 CA–II^{2}H$^\beta$, 0.68 Å. During the restrained simulation, no stable hydrogen bonds are observed. Again, this is in contrast to the low-temperature coefficient for the Phe^{2}H^N.

Table 5. Intraresidual Distances Calculated from NOESY Spectra of SP1 in DMSO and SP2 in DMSO and H_2O[a]

	SP1		SP2	
atoms	major	minor	DMSO	H_2O
Gly^{0}H^N Gly^{0}H$^{\alpha 1}$	2.7	2.5		
Gly^{0}H^N Gly^{0}H$^{\alpha 2}$	2.4	2.5		
Arg^{1}H^N Arg^{1}H$^\alpha$	*b*	2.7	3.1	2.9
Arg^{1}H^N Arg^{1}H$^{\beta 1}$	2.9		3.0 }	2.8[c]
Arg^{1}H^N Arg^{1}H$^{\beta 2}$	2.6	*b*	2.9 }	
Arg^{1}H^N Arg^{1}H$^{\gamma 1}$	3.1	*b*	*b*	2.8
Arg^{1}H^N Arg^{1}H$^{\gamma 2}$	3.0	*b*	*b*	3.2
Arg^{1}H$^\alpha$ Arg^{1}H$^{\beta 1}$	2.5	2.6	2.8 }	2.7[c]
Arg^{1}H$^\alpha$ Arg^{1}H$^{\beta 2}$	2.7	*b*	3.0 }	
Arg^{1}H$^\alpha$ Arg^{1}H$^{\gamma 1}$	*b*		*b*	2.9
Arg^{1}H$^\alpha$ Arg^{1}H$^{\gamma 2}$	*b*		*b*	2.8
Arg^{1}H$^\alpha$ Arg^{1}H$^\delta$	3.9		3.9	3.6
Arg^{1}H$^{\beta 1}$ Arg^{1}H$^\delta$	3.2	3.5	3.3	*b*
Arg^{1}H$^\beta$ Arg^{1}H$^{\gamma 1}$	*b*	*b*	*b*	2.8
Arg^{1}H$^\delta$ Arg^{1}H$^{\gamma 2}$	*b*	*b*	*b*	2.9
Phe^{2}H^N Phe^{2}H$^\alpha$	2.7	2.4	3.2	3.1
Phe^{2}H^N Phe^{2}H$^{\beta 1}$	3.4		4.4	4.5
Phe^{2}H^N Phe^{2}H$^{\beta 2}$	2.6	2.7	3.2	3.1
Phe^{2}H$^\alpha$ Phe^{2}H$^{\beta 1}$	2.5	2.6	2.7	2.6
Phe^{2}H$^\alpha$ Phe^{2}H$^{\beta 2}$	2.7	2.8	2.8	2.7
Phe^{3}H^N Phe^{3}H$^\alpha$	2.8	2.6	2.4	*b*
Phe^{3}H^N Phe^{3}H$^{\beta 1}$	2.8	2.7	2.8	2.8
Phe^{3}H^N Phe^{3}H$^{\beta 2}$	2.9	2.5	2.7	2.7
Phe^{3}H$^\alpha$ Phe^{3}H$^{\beta 1}$	2.6	2.4	2.8	2.6
Phe^{3}H$^\alpha$ Phe^{3}H$^{\beta 2}$	2.6	2.7	2.9	2.7
Leu^{5}H^N Leu^{5}H$^\alpha$	*b*	2.5	2.7	2.8
Leu^{5}H^N Leu^{5}H$^\beta$	2.7	2.7	3.1	2.6
Leu^{5}H^N Leu^{5}H$^\gamma$	3.2	3.3		
Met^{6}H^N Met^{6}H$^\alpha$	*b*	2.4	2.6	2.9
Met^{6}H^N Met^{6}H$^{\beta 2}$	3.2			*b*
Met^{6}H^N Met^{6}H$^{\gamma 1}$				3.3
Met^{6}H^N Met^{6}H$^{\gamma 2}$				3.3
Met^{6}H$^\alpha$ Met^{6}H$^{\beta 1}$				3.0
Met^{6}H$^\alpha$ Met^{6}H$^{\beta 2}$				2.9
II H^N II H$^{\alpha 1}$	2.8 }	2.8[c]	3.3	2.8
II H^N II H$^{\alpha 2}$	2.3 }		2.9	2.7
II H^N II H$^{\beta 1}$ }	3.4[c]		3.3	
II H^N II H$^{\beta 2}$ }			3.4	3.3
II H^N II H$^\gamma$			*b*	3.5
II H$^{\alpha 1}$ II H$^{\beta 1}$	*b*	*b*	2.7	*b*
II H$^{\alpha 1}$ II H$^{\beta 2}$	*b*	*b*	2.8	2.5
II H$^{\alpha 2}$ II H$^{\beta 1}$ }	1.9[d]	*b*	2.7	2.6
II H$^{\alpha 2}$ II H$^{\beta 2}$ }		*b*	2.8	*b*
II H$^{\beta 1}$ II H$^\gamma$			*b*	2.9
II H$^{\beta 2}$ II H$^\gamma$			*b*	2.8

[a] Distances are in Å. [b] Distances could not be determined because of the signal overlap. [c] H$^\beta$ are overlapped. [d] H$^\beta$ are overlapped, and distance is not used in the calculations.

The average structure, partially energy minimized, is given in Figure 3, bottom.

The free MD simulation of SP2 in DMSO illustrates that the conformation is stable and very few conformational changes take place (Table 7). The largest change of an averaged dihedral angle is less than 30°.

For the water simulation of SP2, the conformation obtained at the end of the restrained simulation (in DMSO) was used as a starting structure. The restraints from the water investigation were almost completely fulfilled by the DMSO conformation. The average dihedral angles (data not given) are almost identical with those given for DMSO. This finding is not surprising considering the small difference in the experimental observations.

Floating chiralities with both NOE and coupling constants as restraints was used for the β-methylene protons of the arginine and two phenylalanines. The diastereotopic assignments, given in Table 2, are unambiguous for all except one of the side chains. Carrying out additional simulations with different starting side-chain orientations produces the same results. The one that is not consistently

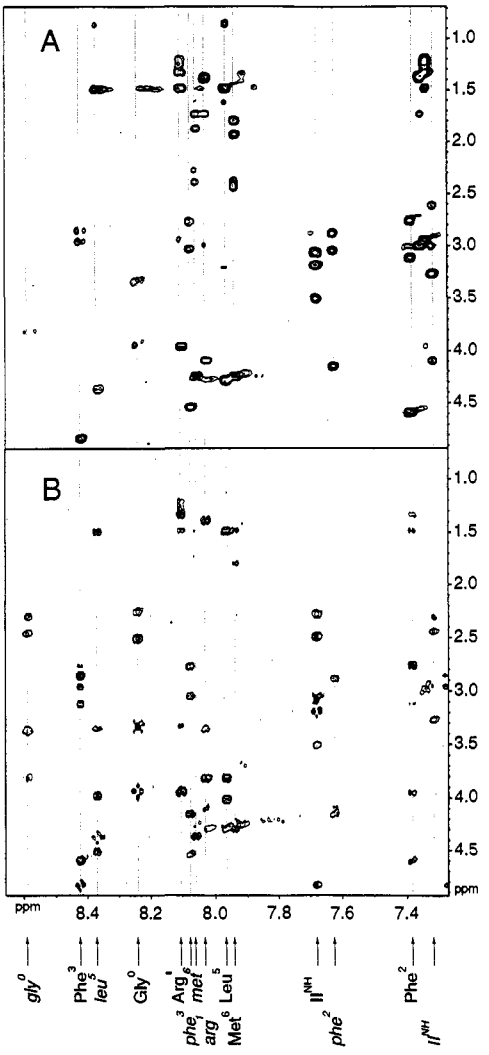

Figure 2. Expanded portion of the aliphatic to amide region of (A) TOCSY and (B) NOESY spectra of SP1 measured at 600 MHz in DMSO. The amide resonances for both of the spectrum are labeled below. The resonances from the trans isomer are shown as bold and those from the cis isomer in italics.

reproduced is the Phe^3 side chain of SP1. The NOE and coupling constant data are consistent with rotations or conformational flexibility. During the simulation, after the floating chiralities was turned off, the 180° and 60° rotamers are populated with almost equal populations, producing the unlikely average dihedral angle of 130°.

Discussion

The comparison of the two analogs examined here along with the two related compounds previously examined, cyclo[-$(CH_2)_m$-NH-CO-$(CH_2)_n$-CO-Arg^1-Phe^2-Phe^3-N-]-CH_2-CO-Leu-Met-NH_2 where m,n = 3,2 and 3,3 (SP3 and SP4 in Figure 1),[4] should allow for insight into the conformational requirements for binding and activity at the NK_1 receptor.

It is important to note that only the N-terminal portion of these molecules is constrained; the C-terminal half is linear, conformationally free, and can adopt many conformations. This is indicated by the difference in the NMR data; there are many more NOEs (i.e., restraints) for the cyclic portion of the molecule. Therefore, in the comparison of the series of backbone-cyclized SP analogs, only the N-terminal portion will be discussed. From the analysis of linear analogs of SP, it has been postulated that the Gly is necessary to allow for the additional conformational freedom of the C-terminal portion of the molecule.[1,2]

The inactivity of SP1 appears to arise from the introduction of too much constraint into the ring system. The ring system which is of the same size of the other analog (20 members) adopts a bent, folded conformation. This is to be contrasted with the relatively extended conformation of the ring system found for the three biologically active analogs. This ring conformation has a great effect on the arrangement of the biologically important side chains of the two phenylalanines and arginine. For example, the distance between the Arg and Phe^2 side chains (using the β carbon) are 4.8 and 7.0 Å for SP1 and SP2, respectively. The distance between the two phenylalanine side chains is 6.5 and 8.4 Å for SP1 and SP2, respectively. To illustrate these differences, the three residues of the ring system have been superimposed for the active and inactive analogs in Figure 4.

The overall topology of the three active analogs is similar in this region. There are small differences in the ϕ and ψ dihedral angles or the side-chain rotamers, but the general arrangement of these important side chains is similar. It is important to note that upon binding to the receptor, significant conformational changes can take place, even for cyclic molecules.[11,12] Therefore, it is highly probable that side chains can rotate 120° to adopt another rotamer or small changes in the dihedral angles can take place. On the other hand, it seems physically impossible for the inactive analog (SP1) to adopt a conformation with the three residues in a topological arrangement similar to that of the three active analogs.

Recently, it was found that in the case of G-protein-coupled receptors, i.e., the tachykinin receptors NK-1[13-15] and NK-2,[15] the angiotensin receptor AT_1,[15] and the CCK gastrin receptor,[16] nonpeptide antagonists interact with different locations on the receptor than their corresponding

Table 6. Proton Vicinal Coupling Constants of SP1 in DMSO and SP2 in DMSO and H_2O (or D_2O)[a]

	$^3J_{NHH^\alpha}$				$^3J_{H^\alpha H^\alpha}$			
	SP1		SP2		SP1		SP2	
residue	major	minor	DMSO	H_2O	major[d]	minor[d]	DMSO[d]	D_2O[d]
Gly^0	6.2, 4.9[d]	6.7, 6.3[d]						
Arg^1	8.6	9.0	7.3	6.0	5.8, 8.8	4.9, 8.4	6.3, 8.8	*b*
Phe^2	9.1	8.3	8.2	8.8	4.9, 10.1	5.3, 9.7	4.2, 8.1	5.1, 9.2
Phe^3	6.6	8.5	8.0	7.4	6.2, 8.4	4.5, 11.0	6.8, 8.8	6.4, 8.5
Leu^5	8.0	8.1	7.7	6.4				
Met^6	8.1	8.1	8.4	7.2	*b*	*b*	4.7, 8.8	5.1, 9.5
II	6.5, 5.7[d]	11.3[c]	6.9, 4.7[d]	6.0, 6.0[d]	*b*	*b*	*b*	*b*

[a] Couplings are given in Hz. The accuracy of $^3J(NH,H^\alpha)$ couplings of SP2 determined in H_2O from 1D proton spectra is 0.5 Hz. Other couplings were determined from P.E.COSY spectra with the accuracy of 0.3 Hz. [b] Couplings could not be measured because of the signal overlap. [c] H^α are chemically equivalent, and one large coupling is observed. [d] The low-field protons are listed first.

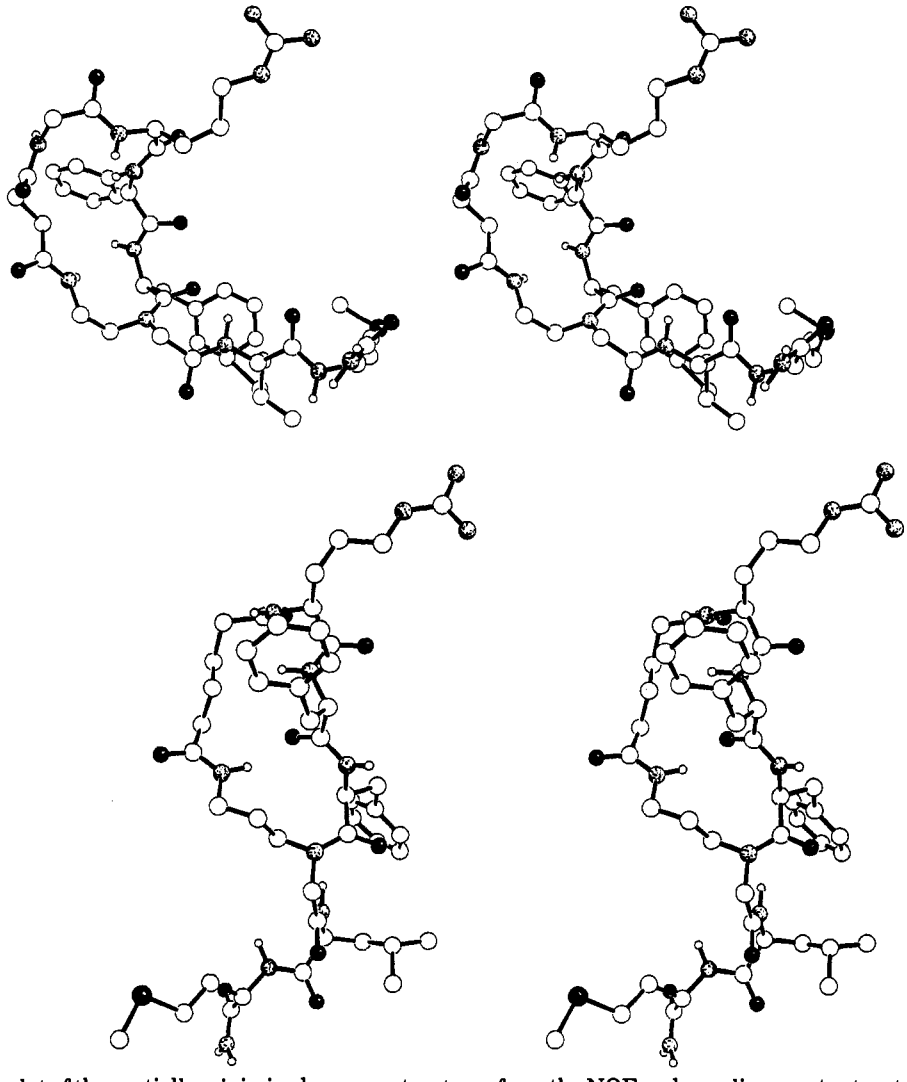

Figure 3. Stereoplot of the partially minimized average structures from the NOE and coupling constant restrained molecular dynamics in DMSO of (top) SP1 trans isomer and (bottom) SP2.

agonists. Moreover, by using point-mutated and chimeric receptors, it was found that in the case of the tachykinin receptors NK-1 and NK-2 and the angiotensin receptor AT_1, the binding of the nonpeptide antagonists could be separated from the binding of the peptide agonists.[15] On the basis of these findings, a common molecular mechanism for the action of the nonpeptide antagonists to G-protein-coupled receptors was suggested.[13,15] All interfere with the correct packing of two adjacent trans membrane-helices which are crucial for G-protein coupling, signal transduction, and allosteric induction of the high-affinity state of the receptor.

From these findings, we can conclude that the structure of nonpeptide antagonists could not be used for the elucidation of the bioactive conformation of their corresponding agonists, since they bind to different locations on the receptor. Since the 3D structure of the receptor–agonist complex of any neuropeptide has not been determined experimentally up till now, one has to find alternative routes to determine the bioactive conformation of these important peptides.

Our approach, as demonstrated in this article, consists of elucidating conformational features of the bioactive conformation by comparing the 3D structures of active and nonactive agonists derived from NMR and MD calculations. The fact that analog SP2 gave the same experimental parameters in both DMSO and water establishes the validity of the conformational analysis.

The three active analogs and one nonactive analog used in this comparison were selected on the basis of their high structural similarity: they differ from each other in minute structural elements located in regions which are not essential for receptor interaction (the external ring formed by backbone cyclization). Thus, the ring conformation of these analogs could be compared to elucidate conformational features of the bioactive conformation. These results can also explain the loss of activity of analog SP1. It could be attributed to excess conformational constraints which preclude the adoption of the bioactive conformation on all three tachykinin receptors.

Conclusions

The conformational analysis of two backbone-cyclized analogs of substance P in DMSO and water has been described. These conformations, along with those of two related molecules previously examined, have been used to explain the binding and activity at the NK-1 receptor. The relative, topological arrangement of the two phenylalanines plays an important role.

In addition, the use of homonuclear coupling constants in the method of floating chirality has been introduced to facilitate the diastereotopic assignment of methylene

Table 7. Average Dihedral Angles from Restrained (NOEs and coupling constants) are Free Molecular Dynamics Simulations of SP1 and SP2 in DMSO[a]

	SP1		SP2	
torsion	NOE	free	NOE	free
Gly^0 ϕ	120	116		
ψ	-71	-77		
Arg^1 ϕ	-98	-104	-102	-74
ψ	-18	-74	-30	-28
χ_1	-149	-108	-117	-130
Phe^2 ϕ	80	-138	-98	-105
ψ	141	-68	151	141
χ_1	-135	-161	-34	-44
Phe^3 ϕ	33	-126	-127	-116
ψ	108	144	96	105
χ_1	130	162	-171	-170
Gly^4 ϕ	-59	-53	-85	-60
ψ	88	120	-4	-14
Leu^5 ϕ	-155	-133	35	41
ψ	148	118	61	43
Met^6 ϕ	69	61	-92	-127
ψ	45	-61	141	138
I[b] χ_1	103	104	-107	-135
χ_2	81	89	76	74
χ_3	-178	-173	178	-175
χ_4			-170	-167
χ_5			-92	-86
II[b] χ_1	-177	-154	-164	-167
χ_2	88	68	-74	-79
χ_3	-101	-102	-180	177
χ_4			-88	-108

[a] Values are given in degrees. [b] The definitions of the torsions of the bridging regions are as follows. SP1 (fragment I): χ_1, NH(Gly^0)-CO-CH_2-CH_2; χ_2, CO-CH_2-CH_2-CO; χ_3, CH_2-CH_2-CO-NH(II). SP1 (fragment II): χ_1, CO(I)-NH-CH_2-CH_2; χ_2, NH-CH_2-CH_2-N(Gly^4); χ_3, CH_2-CH_2-N(Gly^4)-CO(Phe^3). SP2 (fragment I): χ_1, NH(Arg^1)-CO-CH_2-CH_2; χ_2, CO-CH_2-CH_2-CH_2; χ_3, CH_2-CH_2-CH_2-CH_2; χ_4, CH_2-CH_2-CH_2-CO; χ_5, CH_2-CH_2-CO-NH(II). SP2 (fragment II): χ_1, CO(I)-NH-CH_2-CH_2; χ_2, NH-CH_2-CH_2-CH_2; χ_3, CH_2-CH_2-CH_2-N(Gly^4); χ_4, CH_2-CH_2-N(Gly^4)-CO(Phe^3).

protons. The use of both NOEs and coupling constants is an important method for systems in low concentration, where heteronuclear coupling constants are not possible to measure.

On the basis of the results described in this article, we suggest that the backbone dihedral angles of the sequence -Phe-Phe- of SP required for activation of the NK-1 receptor are those shown in Table 7.

Experimental Methods

The synthesis, characterization, and biological activity of peptides SP1, SP2, SP3, and SP4 are described in ref 17.

Nuclear Magnetic Resonance. Proton and carbon spectra of SP1 and SP2 were recorded on Bruker AMX-600 and AMX-500 spectrometers. The sample concentrations were 0.7 mM in DMSO and 3.2 mM in D_2O or 90% H_2O/10% D_2O solutions. Spectra of SP1 and SP2 were recorded at 310 and 300 K, respectively. Temperature coefficients of the amide protons in DMSO were measured in the range from 300 to 340 K.

The NOESY[18] and ROESY[19-21] spectra were recorded with 4096 data points in the t_2 dimension, 512 points in the t_1 dimension, 96–128 scans, and a relaxation delay of 1.3 s. The mixing time was 150 ms, with the exception of a ROESY experiment of SP1 in DMSO where 200 ms was used. A field strength of 3 kHz was used for the spin locking of the ROESY. Spectral widths of 7246, 6024, 6250, and 5556 Hz were used in both dimensions for SP1 in DMSO and for SP2 in DMSO, 90% H_2O/10% D_2O, and D_2O, respectively. For measurements in water, a jump-and-return sequence[22] and a spin-lock pulse[23] were applied before acquisition in the NOESY and ROESY experiments, respectively. Data were zero-filled two times and apodizied with a squared sine bell function shifted by $\pi/2$ in both dimensions. The distances of SP1 and SP2 in DMSO were determined from NOESY spectra and of SP2 in D_2O and 90% H_2O/10% D_2O from ROESY spectra. The integral intensities of cross-peaks were measured by the integration routine within the UXNMR program.

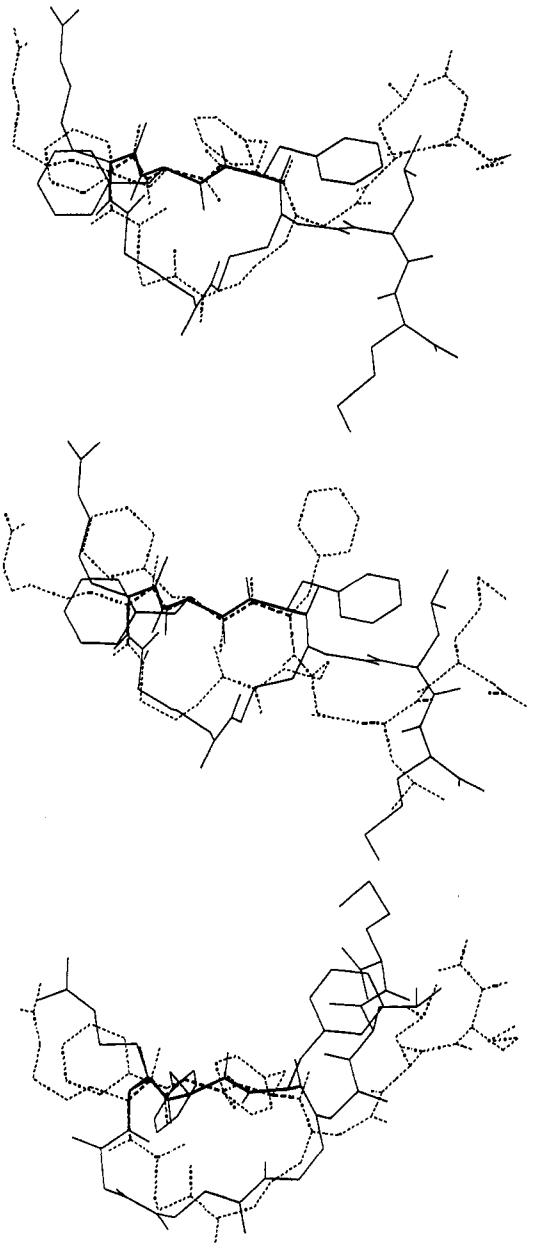

Figure 4. Superposition of the substance P analogs (top) SP2 (solid line) and SP3 (dash line), (middle) SP2 (solid line) and SP4 (dash line), and (bottom) SP1 (solid line) and SP3 (dash line). The three residues of the cyclic portion of the molecules (Arg^1, Phe^2, and Phe^3 indicated with bold line) have been used in the superpositions. The similarities of the spatial arrangement of the side chains for the active analogs are indicated (top and middle). This is to be contrasted with the inactive analog (SP1) shown at the bottom.

The TOCSY[24,25] spectra were recorded with an MLEV-17[26] mixing sequence of 60 ms, a 10-kHz spin-lock field strength, 4096 data points in t_2, 16–64 scans, 322–512 points in the t_1 dimension, and a relaxation delay of 0.7–1.3 s. Spectral widths in both dimensions were 7246, 6024, 6250, and 5556 Hz for SP1 in DMSO and for SP2 in DMSO, 90% H_2O/10% D_2O, and D_2O, respectively. For water suppression, a jump-and-return sequence was used before acquisition. Data were zero-filled two times and apodizied with a squared sine bell function shifted by $\pi/2$ in both dimensions.

The P.E.COSY[27] spectra were recorded with 8192 data points in t_2, 64 scans, 600–880 points in t_1, and a relaxation delay of 1.2 s. Spectral widths in both dimensions were 7246, 6024, and 5556

Hz for SP1 in DMSO and for SP2 in DMSO and D_2O, respectively. The reference 1D proton spectrum was recorded with 16 384 points. The relaxation delay was equal to the relaxation delay of the 2D experiment reduced by the acquisition time of the 2D experiment. The delay before acquisition was equal to $2\tau_p/\pi + 2\ \mu s$, where τ_p is the length of a 37° proton pulse. The reference spectrum was subtracted from the 2D spectrum before Fourier transformation. Data were zero-filled two times and apodizied with a squared sine bell function shifted by $\pi/3$ in both dimensions. The slices containing coupling information were extracted from 2D spectra, inverse Fourier transformed, zero-filled, and processed with a squared sine bell function shifted by $\pi/2$. The estimated accuracy of the couplings is 0.3 Hz.

The ^1H and ^{13}C HMQC[28] spectrum of SP1 was recorded with 4096 data points in t_2, 128 scans, 512 points in t_1, a spectral width of 7246 Hz in the t_2 dimension, and a spectral width of 10 563 Hz in the t_1 dimension. The optimum delay for the BIRD sequence[29] used for presaturation of protons bonded to ^{12}C was 190 ms. The ^1H and ^{13}C HMQC spectra of SP2 were recorded with 2048 data points in t_2, 64–128 scans, 256–344 points in t_1, and a spectral width of 8928 Hz in the t_1 dimension. The spectral width in t_2 was 6024 Hz in DMSO and 5556 Hz in D_2O. The optimum delays for the BIRD sequence were 200 and 500 ms in DMSO and D_2O, respectively. Spectra were zero-filled two times and apodizied with a squared sine bell function shifted by $\pi/2$ in both dimensions.

Computer Simulations. All of the MD simulations were carried out in DMSO[30] and H_2O (SPC model). The DMSO is described by a four-point model with a united atom used for the CH_3 methyl group. The solvent is considered rigid with the geometry maintained by the application of SHAKE.[31] A detailed description of the use of DMSO in MD simulations has been published.[30,32] All of the simulations were carried out with the GROMOS program.[33]

The two SP molecules were built using the InsightII program (Biosym Technologies). The structures were partially minimized (200 steps of steepest descents) and then placed in a periodic truncated octahedron of DMSO with a peptide-to-edge distance of 10 Å. The system was minimized for 1000 steps of steepest descents. For the cis configurational isomer of the SP1 analog, a potential was placed on the peptide bond between Phe^3 and Gly^4 to obtain a cis orientation.

The MD simulations were carried out with the following procedure: (1) 20 ps at 500 K with $k_J = 0.25$, (2) 20 ps at 300 K with $k_J = 0.50$, and (3) 240 ps at 300 K with $k_J = 1.0$, where k_J is the force constant for the application of the coupling constant restraints in units of kcal mol^{-1} Hz^{-2}. The temperature was maintained by a weak coupling to a temperature bath.[34] The force constant for the NOEs was maintained at 3000 kcal mol^{-1} nm^{-2}. The distance restraints were applied in the standard manner, with the upper and lower restraints calculated as +10% and −10% of the distance from the NOE calibration. A step size of 2 fs, employing the SHAKE algorithm,[31] was used with the nonbonded interactions updated every 25 steps with a cutoff radius of 1.0 nm. The last 100 ps of the simulation was used for analysis. Free MD was carried out by removing the NOE and coupling constant restraints and continuing the simulation for 140 ps. The last 100 ps of the free MD was used for analysis.

The application of the constraints from the coupling constants has been previously described.[6,35] The penalty function is similar to that commonly used for NOE restraints:

$$E_J = {}^1/_2 k_J (J - J_{exp})^2 \quad (1)$$

where k_J is the force constant, E_J is the energy of the penalty function, and J and J_{exp} are the coupling constants calcualted from the dihedral angle and the experimental value, respectively. The coupling constant is calculated from the dihedral subtended by the coupled atoms, Θ, using Karplus equations:[36]

$$^3J = A\cos^2\Theta + B\cos\Theta + C \quad (2)$$

where the coefficients A, B, and C have been empirically adjusted for dihedral torsions involving different atoms. The coupling constant restraints were applied following procedures previously described with the exception of the $^3J_{H^\alpha H^\beta}$ couplings which are modified since the diastereotopic assignments are not available.

Previously, the forces from the experimental restraints were applied to the heavy atoms involved in the dihedral angles (i.e., for the $^3J_{H^\alpha H^\beta}$ coupling containing information about the χ_1 torsion, the forces are transferred to the heavy atoms, N–CA–CB–CG, defining the torsion). However, this requires the appropriate phase shift from the proton–proton torsion (Θ) to the heavy atom torsion (χ_1) which depends on the diastereotopic assignment. To avoid this problem, an all-atom force field must be used and the forces developed from the application of the coupling constant restraints must be applied to the hydrogen atoms. To accomplish this, protons were added to the C^α and C^β atoms since GROMOS uses the united-atom approach. Bond lengths and bond angles were taken from standard published values for all-atom force fields. The protons are assigned a partial charge of 0.1 and the carbons −0.1 for each proton attached. The mass of the carbons was reduced appropriately from the united-atom value. The nonbonded parameters (Lennard–Jones) were not modified. It is important to note that the nonbonded parameters for hydrogen are zero in most all-atom force fields.

The floating chirality[5] was obtained by adjusting the force constants for the following angles: CA–CB–HB1, CA–CB–HB2, CG–CB–HB1, CG–CB–HB2, and HB1–CB–HB2. During the initial portion of the simulation (5 ps), the force constant for these angles was set to 0. The force constants were then slowly increased (5 ps of simulation was carried out with the force constants set to 0, 3.5, and 35 kcal mol^{-1} deg^{-2}) back to the standard value of 350 kcal mol^{-1} deg^{-2}. The calculations were carried out on a Silicon Graphics 4D/240SX.

Acknowledgment. The German-Israel Foundation (GIF) for Scientific Research, The Deutsche Forschungsgemeinschaft, Peptor Co., and the Fonds der Chemischen Industrie are gratefully acknowledged for financial support. S.G.G. acknowledges support from the Ministry of Science and Technology of Slovenia.

References

(1) Gilon, C.; Halle, D.; Chorev, M.; Selinger, Z.; Byk, G. Backbone cyclization: a new method for conferring conformational constraint on peptides. *Biopolymers* **1991**, *31*, 745–750.
(2) (a) Wormser, U.; Laufer, R.; Hart, Y.; Chorev, M.; Gilon, C.; Selinger, Z. Highly selective agonists for substance P receptor subtypes. *EMBO J.* **1986**, *5*, 2805–2809. (b) Livian-Teitelbaum, D.; Kolodny, N.; Chorev, M.; Selinger, Z.; Gilon, C. ^1H-NMR studies of receptor-selective substance P analogues reveal distinct predominant conformations in DMSO-d_6. *Biopolymers* **1989**, *28*, 51–64.
(3) Kessler, H. Conformation and biological activity of cyclic peptides. *Angew. Chem., Int. Ed. Engl.* **1982**, *21*, 512–523.
(4) Saulitis, J.; Mierke, D. F.; Byk, G.; Gilon, C.; Kessler, H. Conformation of cyclic analogues of substance P: NMR and molecular dynamics in dimethyl sulfoxide. *J. Am. Chem. Soc.* **1992**, *114*, 4818–4827.
(5) Weber, P. L.; Morrison, R.; Hare, D. Determining stereo-specific ^1H nuclear magnetic resonance assignments from distance geometry calculations. *J. Mol. Biol.* **1988**, *204*, 483–487.
(6) Mierke, D. F.; Kessler, H. Combined use of homo- and heteronuclear coupling constants as restraints in molecular dynamics simulations. *Biopolymers* **1992**, *32*, 1277–1282.
(7) Eberstadt, M.; Mierke, D. F.; Kŏck, M.; Kessler, H. Peptide conformation from coupling constants: scalar couplings as restraints in MD simulations. *Helv. Chim. Acta* **1992**, *75*, 2583–2592.
(8) Mierke, D. F.; Golic Grdadolnik, S.; Kessler, H. Use of one-bond C^α-H^α coupling constants as restraints in MD simulations. *J. Am. Chem. Soc.* **1992**, *114*, 8283–8284.
(9) Wüthrich, K. *NMR of Proteins and Nucleic Acids*; John Wiley: New York, 1986.
(10) Kessler, H.; Bermel, W.; Müller, A.; Pook, K. H. Modern nuclear magnetic resonance spectroscopy of peptides. In *The Peptides: Analysis, Synthesis, Biology*, 7th ed.: Udenfriend, S., Meinhofer, J., Hruby, V., Eds.; Academic Press: Orlando, 1985; pp 437–473.

(11) Weber, C.; Wider, G.; von Freyberg, B.; Traber, R.; Braun, W.; Widmer, H.; Wüthrich, K. The NMR structure of cyclosporin A bound to cyclophilin in aqueous solution. *Biochemistry* **1991**, *30*, 6563–6574.
(12) Fesik, S. W.; Gampe, R. T.; Eaton, H. L., Jr.; Gemmecker, G.; Olejniczak, E. T.; Neri, P.; Holzman, T. F.; Egan, D. A.; Edalji, R.; Simmer, R.; Helfrich, R.; Hochlowski, J.; Jackson, M. NMR studies of [U-^{13}C] cyclosporin A bound to cyclophilin: bound conformation and portions of cyclosporin involved in binding. *Biochemistry* **1991**, *30*, 6574–6583.
(13) Gether, U.; Johansen, T. E.; Snider, M. R.; Lowe, J. A., III; Nakanishi, S.; Schwartz, T. W. Different binding epitopes on the NK_1 receptor for substance P and a non-peptide antagonist. *Nature* **1993**, *362*, 345–348.
(14) Fong, T. M.; Cascieri, M. A.; Yu, H.; Bansal, A.; Swain, C.; Strader, C. D. Amino-aromatic interaction between histidine 197 of neurokinin-1 receptor and CP 96345. *Nature* **1993**, *362*, 350–353.
(15) Schwartz, T. W.; Gether, U.; Schambye, H. T.; Nielsen, S. M.; Elling, C.; Jensen, C.; Zoffman, S.; Hjorth, S. *206th ACS National Meeting*; **1993**, Abstract, p 263.
(16) Beinborn, M.; Lee, Y.-M.; McBride, E. W.; Quinn, S. M.; Kopin, A. S. A single amino acid of the cholecystokinin-B/gastrin receptor determines specificity for non-peptide antagonists. *Nature* **1993**, *362*, 348–351.
(17) Gilon, C.; Zeltzer, I.; Rashti-Bahar, V.; Muller, D.; Bitan, G.; Halle, D.; Bar-Akiva, G.; Selinger, Z.; Byk, G. Backbone cyclization as a tool for imposing conformational constraint on peptides. In *Peptide Chemistry 1992*; Yanaihara, N., Ed.; Escom: Leiden, 1993; pp 482–485.
(18) Jeener, J.; Meier, B. H.; Bachmann, P.; Ernst, R. R. Investigation of exchange processes by two-dimensional NMR spectroscopy. *J. Chem. Phys.* **1979**, *71*, 4546–4553.
(19) Kessler, H.; Griesinger, C.; Kerssebaum, R.; Wagner, K.; Ernst, R. R. Separation of cross-relaxation and J cross-peaks in 2D rotating-frame NMR spectroscopy. *J. Am. Chem. Soc.* **1987**, *109*, 607–609.
(20) Bothner-By, A. A.; Stephens, R. L.; Lee, J.; Warren, C. D.; Jeanloz, R. W. Structure determination of a tetrasaccharide: transient nuclear Ovehauser effects in the rotating frame. *J. Am. Chem. Soc.* **1984**, *106*, 811–813.
(21) Bax, A.; Davies, D. G. Practical aspects of two-dimensional transverse NOE spectroscopy. *J. Magn. Reson.* **1985**, *63*, 207–213.
(22) Plateau, P.; Gueron, M. Exchangeable proton NMR without baseline distortion, using new strong-pulse sequences. *J. Am. Chem. Soc.* **1992**, *104*, 7310–7311.
(23) Otting, G.; Liepinsh, E.; Farmer, B. T., II; Wüthrich K. Protein hydration studied with homonuclear 3D ^{1}H NMR experiments. *J. Biomol. NMR* **1991**, *1*, 209–215.
(24) Braunschweiler, L.; Ernst, R. R. Coherence transfer by isotropic mixing: application to proton correlation spectroscopy. *J. Magn. Reson.* **1983**, *53*, 521–528.
(25) Bax, B.; Davis, D. G. Assignment of complex ^{1}H NMR spectra via two-dimensional homonuclear Hartmann-Hahn spectroscopy. *J. Am. Chem. Soc.* **1985**, *107*, 2820–2821.
(26) Bax, B.; Davis, D. G. MLEV-17-based two-dimensional homonuclear magnetization transfer spectroscopy. *J. Magn. Reson.* **1985**, *65*, 355–360.
(27) Mueller, L. P.E.COSY, a simple alternative to E.COSY. *J. Magn. Reson.* **1987**, *72*, 191–196.
(28) Mueller, L. Sensitivity enhanced detection of weak nuclei using heteronuclear multiple quantum coherence. *J. Am. Chem. Soc.* **1979**, *101*, 4481–4484.
(29) Garbow, J. R.; Weitekamp, D. F.; Pines, A. Bilinear rotation decoupling of homonuclear scalar interactions. *Chem. Phys. Lett.* **1982**, *93*, 504–509.
(30) Mierke, D. F.; Kessler, H. Molecular dynamics with dimethyl sulfoxide as a solvent. Conformation of a cyclic hexapeptide. *J. Am. Chem. Soc.* **1991**, *113*, 9466–9470.
(31) Ryckaert, J. P.; Ciccotti, G.; Berendsen, H. J. C. Numerical integration of the cartesian equations of motion of a system with constraints: molecular dynamics of n-alkanes. *J. Comput. Phys.* **1977**, *23*, 327–341.
(32) Kurz, M.; Mierke, D. F.; Kessler, H. Calculation of molecular dynamics for peptides in dimethyl sulfoxide: elimination of vacuum effects. *Angew. Chem., Int. Ed. Engl.* **1992**, *31*, 210–212.
(33) van Gunsteren, W. F.; Berendsen, H. J. C. *Groningen Molecular Simulation Library Manual*; Biomos B. V.: Nijenborgh 16, NL 9747 AG Groningen, 1987.
(34) Berendsen, H. J. C.; Postma, J. P. M.; van Gunsteren, W. F.; DiNola, A.; Haak, J. R. Molecular dynamics with coupling to an external bath. *J. Chem. Phys.* **1984**, *81*, 3684–3690.
(35) Kim, Y.; Prestegard, J. H. Refinement of the NMR structures for acyl carrier protein with scalar coupling data. *Proteins: Struct., Funct., and Genet.* **1990**, *8*, 377–382.
(36) Karplus, M. Vicinal proton coupling in nuclear magnetic resonance. *J. Am. Chem. Soc.* **1963**, *85*, 2870–2871.